JOURNAL OF MATERIALS SCIENCE 32 (1997) 6263–6268

Alumina carbon/epoxy laminates under cyclic loading

D. SHERMAN*
Department of Materials Engineering, Technion-Israel Institute of Technology, Haifa, 32000 Israel

F. A. LECKIE
Department of Mechanical Engineering, University of California, Santa Barbara, CA 93106-5070 USA

The behaviour of alumina carbon/epoxy laminate under cyclic loading was investigated. The laminate was constructed by alternating dense alumina thin plates with unidirectional carbon/epoxy (C/E) prepreg tapes. Several cyclic load amplitudes were applied in unidirectional tension, corresponding to the stresses at onset of cracks in the alumina layers. The experimental results revealed high threshold stresses before damage occurred. These threshold stresses are matched with the stresses at onset of cracks in the alumina layers at static tensile tests. When the maximum stresses exceed this threshold, a very rapid stiffness reduction follows. The rate of loss of stiffness was examined. The short range rate was varied as a function of the maximum stress amplitude, but the long-term rate of loss of stiffness was found to be independent of the maximum stresses. A plastic shakedown mechanism was evident for cracked system undergoing high number of cycles, and is attributed to the nearly elastic plastic feature of the epoxy, the bonding agent between the alumina and the C/E layers.

1. Introduction

Delayed fracture of monolithic structural ceramics both under static and under cyclic loading is attributed to subcritical crack growth. Hence, the fatigue behaviour can be predicted by the crack growth under static loading [1–4]. The growth rate was found to be dependent of K_{max} rather than ΔK, and the subcritical crack growth rate under fatigue conditions can exceed the growth rate under static loading by several orders of magnitude, stress intensity levels being equal. The mechanisms of crack advance were similar in both cases [5].

Fibre composites under cyclic loading have been extensively studied over the last three decades. Highsmith and Reifsnider [6] studied the behaviour of polymeric matrix composites under cyclic loading, demonstrating the loss of stiffness as a function of crack density. Talreja formulated the fatigue life of composites under cyclic loading [7] and Prewo *et al.* [8] described the influence of the existence of a proportional limit in static loading on the progressive loss of stiffness under cyclic fatigue. In ceramic matrix composites (CMCs), no loss of stiffness was observed during cyclic loading when the experimental stresses were below the proportional limit. However, when the composite was tested under cyclic loading above that limit, matrix cracking was the main cause of stiffness reduction [8]. Wang *et al.* [9] have investigated the behaviour of laminated 0/90 SiC reinforced carbon composite under cyclic loading with and without notch. Suresh and co-workers [10] have demonstrated the effect of mechanical fatigue, in tension–tension and in compression–compression, on the damage accumulation in monolithic ceramics and CMCs at room temperature, and also at elevated temperature [11–12]. They observed crack growth even when the stress intensity factor at the crack tip was far below the fracture toughness of the matrix material. A summary of the behaviour of CMCs under cyclic loading can be found in [13].

The behaviour of laminar composites [14] under cyclic loading is under investigation. The behaviour of same composite under static tensile loading was extensively studied by Sherman *et al.* [15–16], and the loss of stiffness as a function of the applied strain was formulated in [17]. In the present work, laminates were tested under three different loading amplitudes, corresponding to the stress–strain relation obtained in static loading, in order to study the effect of the maximum stress level on the behaviour under cyclic loading.

The employment of C/E in this lamellar composite limits the use of the system to relatively low temperatures, and a different system is needed for high temperature applications. The current system gave the

* Author to whom correspondence should be addressed.

0022–2461

opportunity to study the main features of lamellar composites under cyclic loading, and it is expected that the main features of high temperature lamellar composites are similar.

2. Experimental programme

2.1. Materials and processing

The laminate was constructed by alternating thin alumina plates and carbon fibre reinforced epoxy (C/E) prepreg tapes. Coor's $A1_2O_3$ ADS96R with a nominal thickness of 0.635 mm were used as the bulk ceramics. Young's modulus and the strength of alumina are 312 GPa and about 300 MPa, respectively, for the specimens in use [15]. Fiberite HYE 16714 AD C/E prepreg tapes were used as the strong constituent, which served as reinforcement layers. Young's modulus of the C/E is 120 GPa, its strength ranges from 1700 to 2000 GPa.

The processing route of the lamellar composite was developed by Lange *et al.* [14]. Initially, the laminates were constructed at room temperature by alternating thin alumina plates and C/E prepreg sheets. The carbon fibres in this investigation were always unidirectional in the laminate, the alumina layers constituted the outer surfaces. The laminates were put into a vacuum bag and hot pressed for 90 min at a moderate pressure of 350 KPa and a temperature of 135 °C.

Three lay-ups were used for the characterization of the fatigue behaviour. The first was constructed by alternating two alumina layers and one C/E, and was designated as 2A1CE. The second consisted of five alternating layers, three of them being alumina and two C/E (designated as 3A2CE). Using the same notation the third laminate was 4A3CE. The volume fraction of the C/E layers within the laminates ranged between 25 and 30%.

2.2. The specimens and experimental procedure

The tensile specimens were all of a "dog-bone" shape, and 6×55 mm^2 gauge area, as shown in Fig. 1. These specimens were gripped by a compressive load provided by hydraulic grips. Metal tabs were bonded to the wider, upper and lower, portions of the specimens. A reduced area was formed with a 75 mm diameter diamond wheel cutter to ensure uniform uniaxial tensile stress at the gauge length. The large radius ensured low stress concentration.

Tensile tests with "dog-bone" shaped specimens of brittle materials are difficult to perform, mainly due to the bending moment resulting from poor misalignment. On the other hand, "dog-bone" shaped specimens are easy to make, and the strain can be obtained even for highly damaged systems, and the constitutive relationship is therefore readily determined. These features are important, especially in fatigue tests. Special attention was paid to the alignment of the loading system, in order to minimize any bending due to gripping.

The cyclic stress amplitudes were corresponded to the basic stress-strain relationship of the laminate under static tension shown in Fig. 2. Three amplitudes of cyclic stress were applied. In the first, the maximum stress was about half the plateau stress (designated A in Fig. 2). The second amplitude resulted from the maximum cyclic stress being similar to the plateau stress (B in Fig. 2), and in the third type of loading the maximum stress was 300 MPa i.e., appreciably higher than the plateau stress level (C in Fig. 2).

The experimental procedure was as follows. The ratio between the minimum and the maximum stress was kept constant at 0.1. Each test was preceded by an

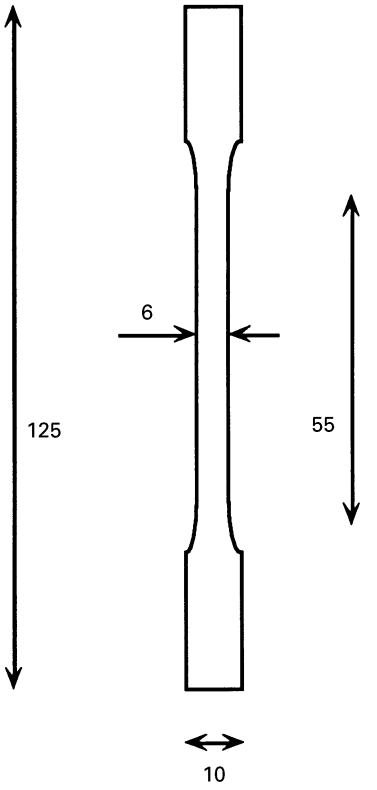

Figure 1 The "dog bone" specimen for fatigue tests.

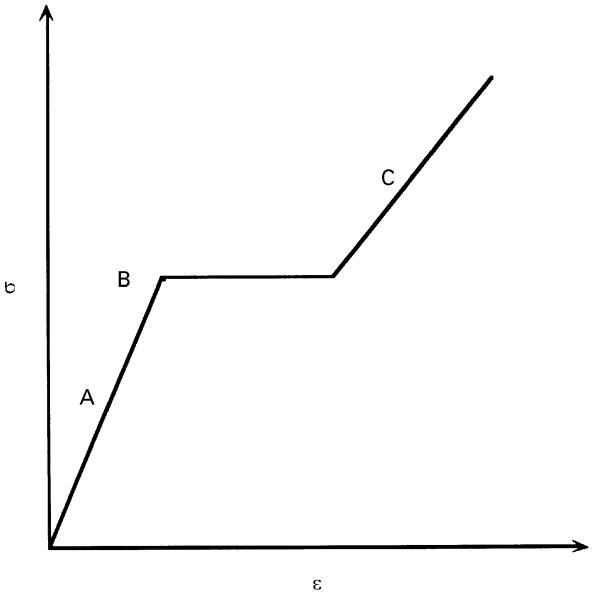

Figure 2 Stress–strain relationship of an alumina C/E laminated system under monotonic tensile stresses.

automatic calculation of the modulus of the specimen involving loading and unloading sequence between the stress levels of 20 and 100 MPa. The procedure comprised automatically calculating the slope between 20 data points of the stress–displacement relationship in this loading and unloading path. The calculated modulus was then calibrated using the "rule of mixtures" modulus.

After the first modulus calculation the specimen was cyclically loaded, the frequency ranging between 8 and 5 Hz. The higher value was used for undamaged systems, the lower frequency for damaged, more compliant systems. The modulus was measured and calculated automatically every specified number of cycles. The sampling data points obtained in the course of the modulus calculations were used to describe the irreversible displacement associated with each modulus, hysteresis loops, and the increase of the displacement during the fatigue life.

3. Observations and results

3.1. Specimens cyclically loaded below the plateau stress level

The first specimen to be cyclically loaded was 3A2CE "dog bone" in which the volume fraction of the C/E was 0.26. A modulus of 262 GPa was obtained using the "rule of mixtures". The plateau stress of such laminate is approximately 205 MPa [15]. Initially, the specimen was cyclically loaded to a maximum stress level of 100 MPa, about half the plateau level (Fig. 2) for 100 500 cycles, during which no damage occurred (Fig. 3a). At this stage it was decided to increase the amplitude to a maximum stress level of 152 MPa. The specimen then was cycled through an additional 74 500 cycles. Again, no damage occurred at the end of this stage, so the amplitude was raised again to a maximum stress level of 172 MPa. The specimen sustained that stress level for an additional 4230 cycles, when the alumina layers started to fracture. The specimen sustained a total of 179 230 cycles without any cracking. Calculations after an additional 2000 cycles showed that the modulus had dropped to 60 GPa.

For the laminate here treated, E_B and E_D are 312 and 120 GPa, respectively. For a volume fraction, f, of 0.26, $\xi = 5.48$ (see Appendix). The predicted elastic modulus at saturation, E_{sat}, was 63 GPa, which is in good agreement with the measured modulus. This calculation indicates that saturation prevailed after 181, 230 cycles.

By the end of the test, after a total of 350 000 cycles, the modulus dropped to 45 MPa. It should be noted that the stiffness of the C/E layers within the laminate was 31 GPa (Fig. 3a). The difference between these two moduli indicates that the cracked alumina layers still carried some load.

The stress–displacement relationship obtained in each modulus calculation as described above, presented an excellent opportunity to study the influence of cyclic loading on the laminate, in particular the stiffness reduction and the irreversible displacement, and to indicate the behaviour of the interface. Four

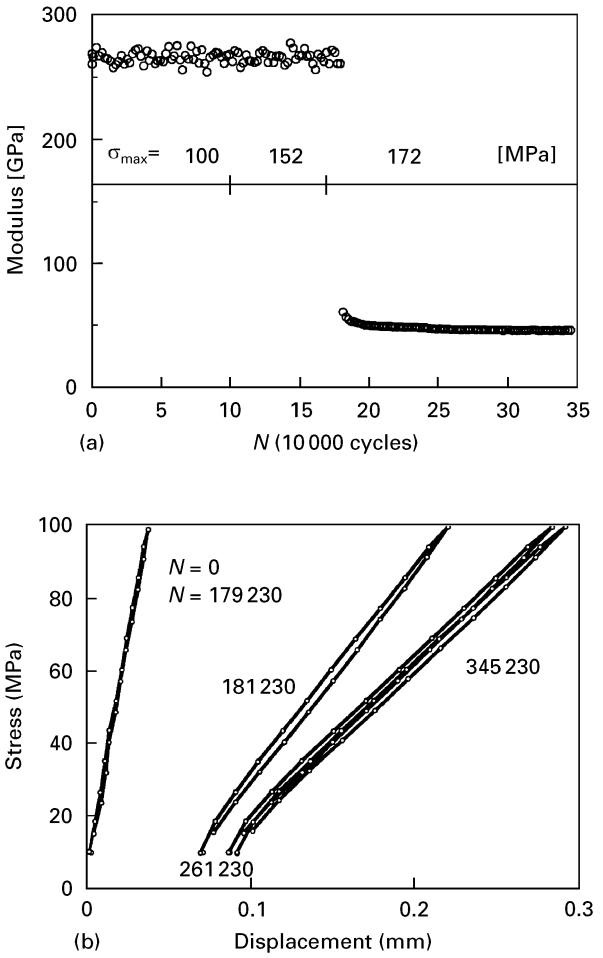

Figure 3 Loss of stiffness as a function of the number of cycles for a 3A2CE laminate under three stress amplitudes (a), and stress–displacement relationship for various numbers of cycles (b).

stress–displacement curves for various numbers of cycles are shown in Fig. 3b. Although the stress amplitudes were increased three times, the stress–displacement curves did not vary after 179 230 cycles, and exhibited no hysteresis. The second stress–displacement curve in Fig. 3b was measured after an additional 2000 cycles and demonstrates the substantial loss of stiffness and large irreversible displacement. Hysteresis behaviour is also evident. The next curve, obtained after a total of 261 230 cycles, exhibits an additional but small loss of stiffness and irreversible displacement. The last stress displacement diagram reveals diminished hysteresis loops and no additional stiffness reduction. The diminished additional irreversible displacement suggests that the effective strain rate of the laminate reduces to zero, namely $\dot{\varepsilon} = 0$, suggests that shakedown mechanism governs the stress–displacement relationship. The relinquished hysteresis loops suggest that the shakedown mechanism is plastic, which is attributed to the interface that behaves as an elastic–plastic material and, therefore, that the interfacial shear strains shakedowns.

From the above test results it was concluded that the alumina C/E laminated system can sustain a high number of cyclic loads without damage, provided the stress level is less than the plateau stress of the laminate. It is postulated that the fatigue threshold stress

in the laminate is relatively high. At a higher maximum stress level the fracture mechanism causes a steep loss of stiffness, and after a few hundreds of cycles, a steady state in the stiffness is reached. Additional cyclic loading at this stage does not cause further loss of stiffness. The stiffness of the C/E layers can always be taken as the lower bound of the modulus drop.

3.2. Specimens cyclically loaded at the plateau stress level

A similar "dog bone" specimen, 4A3CE type, with $f = 0.3$ and a rule of mixtures modulus of 254 GPa, was tested at a maximum stress amplitude of 220 MPa. This stress level coincides with the plateau stress level of the laminate (point A in Fig. 2). The specimen sustained 40 cycles before damage first occurred. The damage then gradually developed. After a total of 70 cycles, the modulus dropped to 100 GPa, and continued to drop until, at a total of 400 cycles, it reached 70 GPa, as shown in Fig. 4a. At a total of 5000 cycles, the modulus had dropped to 65 GPa, and at the end of the test, after a total of 200 000 cycles, the modulus reached 57 GPa. The calculated effective elastic modulus at saturation was 77 GPa (see Appendix), which indicates that a saturation stage in this case prevailed after less than 400 cycles.

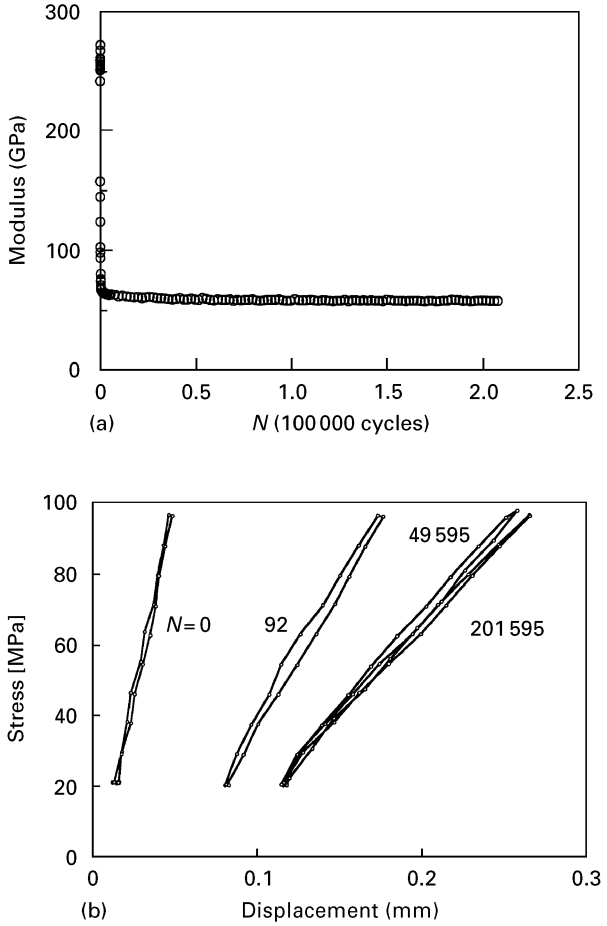

Figure 4 Loss of stiffness as a function of the number of cycles for a 4A3CE laminate. The maximum stress level coincides with the "plateau" stress (a), and the stress–displacement relationship for various numbers of cycles (b). $\sigma_{max} = 220$ MPa.

As with the previous specimen, four stress displacement curves are shown in Fig. 4b, for various numbers of cycles, N. The plastic shakedown mechanism is again evident, as at high number of cycles both the rate of increase of the displacement, and the width of the hysteresis loops reduced. However, the perseverance of the hysteresis loop suggests the elastic–plastic nature of the interface.

3.3. Specimens loaded above the plateau stress level

A 4A3CE "dog bone" specimen ($f = 0.30$), has an undamaged modulus of 254 GPa. The maximum applied amplitude stress was 300 MPa, which was approximately 25% higher than the estimated plateau stress (Fig. 2). As expected, most of the damage, in the form of transverse cracks, occurred in the first cycle, after which the modulus dropped to 90 GPa, as shown in Fig. 5a. Acoustic emissions were clearly heard. After 20 cycles, the modulus had dropped further to 70 GPa. At the end of the experiment, after 100 000 cycles, the modulus was 55 GPa. Note that the modulus of the C/E layers within the laminate was 40 MPa. For this specimen, the effective elastic modulus at saturation (77 GPa) prevailed after a few cycles.

The stress–displacement relationships obtained in each modulus calculation are shown in Fig. 5b. Each curve represents that relationship for a given number of cycles, designated N. The high slope for $N = 0$ was a measure of the high modulus of the undamaged laminate. The other three curves demonstrate that the unloading modulus does not vary during the cyclic loading after saturation has been achieved. The four curves also indicate the increase of the irreversible strain with increasing number of cycles. After 50 000 cycles there was no further change in the stress–displacement curves, which again suggests that a plastic shakedown mechanism governs that relationship. Note the insert of Fig. 5b, which demonstrates a typical damaged laminate at saturation.

The plastic shakedown mechanism observed in these experiments is explained by that mechanism of the epoxy, which serves as the interface and is constrained by the two elastic materials, namely, the alumina and the C/E layers. The plastic shakedown mechanism is responsible for the steady-state behaviour of the unloading modulus after crack saturation. It therefore can be assumed, that these laminates are able to sustain a very high number of cycles after saturation, with no change in modulus and in irreversible strain.

Branches were always associated with cracking in all the above specimens. The spacing between the crack nucleation sites at the end of the cyclic loading was similar to the spacing of the laminates under monotonic loading [11] and was about 5 mm.

3.4. The effect of maximum load on the rate of loss of stiffness

The rate of loss of stiffness as a function of the number of cycles is important for practical applications. It was

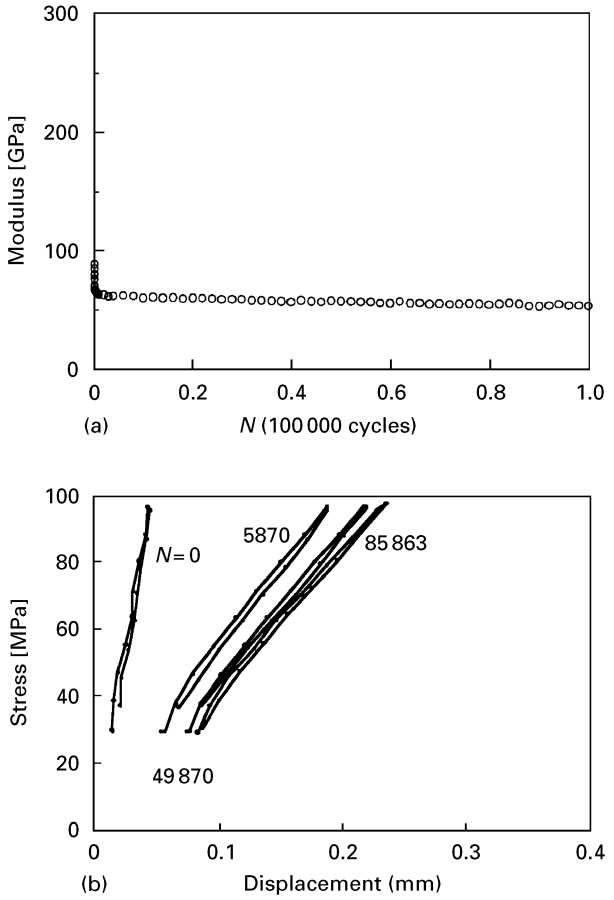

Figure 5 Loss of stiffness as a function of the number of cycles for a 4A3CE laminate under high stress cyclic loading (a), and the stress–displacement relationship for various numbers of cycles (b). The insert of this figure shows a typical damaged laminate at saturation. $\sigma_{max} = 300\,MPa$.

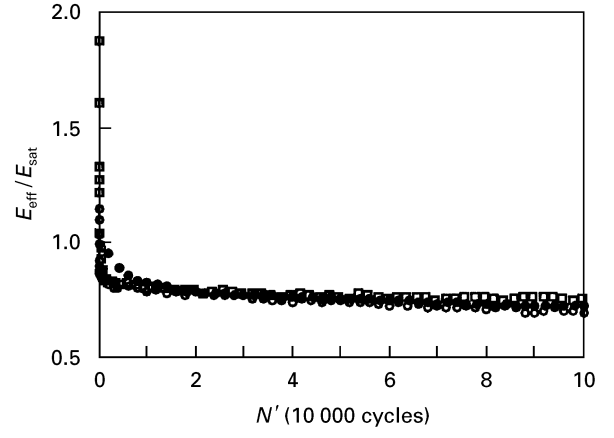

Figure 6 The normalized loss of stiffness as a function of the number of cycles for the three different stress levels. (●) $\sigma_{max} = 172$ MPa; (□) $\sigma_{max} = 220$ MPa; (○) $\sigma_{max} = 300\,MPa$.

examined in the following way: the measured effective elastic modulus, E_{eff}, was normalized by the calculated modulus at saturation, E_{sat}, for each laminate. The normalized moduli were plotted against the accumulated numbers of cycles after the damage was initiated, N, as shown in Fig. 6. It is evident that the short range rate of loss of stiffness is influenced by the maximum applied stresses, but this is true only for several thousands of cycles, afterwards this influence vanishes.

4. Concluding Remarks

The loss of stiffness with increasing numbers of cycles was examined for several lay-ups of the laminated systems. High threshold stresses for the onset of damage was demonstrated, governed by the strength of the alumina layers. The stiffness reduction occurred in small numbers of cycles, negligible from the design point of view. The resulting displacement hysteresis loops reveal a plastic shakedown phenomenon of the interface in highly damaged laminated system.

The calculations of the effective elastic modulus at saturation indicated that the rate of the loss of stiffness depends on the maximum cyclic stresses only for a short range of cycles. For larger numbers of cycles the influence of the maximum stresses on the loss of stiffness disappears. This is associated with the plastic shakedown mechanism.

Acknowledgement

The financial support of the US Air-Force under Grant no. AFOSR-92-0132 to F.A.L. is gratefully acknowledged.

References

1. Y. YAMAUCHI, T. OHJI, W. KANEMATSU, S. ITO and K. KUBO, in "Fracture, Mechanics of Ceramics," Vol. 9, edited by R. C. Bradt, D. P. H. Hasselman, D. Munz, M. Sakai and V. Ya Shevchenko (Plenum Press, New York, 1992) 465–480.
2. U. RAMAMURTY, A. S. KIM, S. SURESH and J. J. PETROVIC, *J. Amer. Ceram. Soc.* **76** (1993) 1953.
3. M. G. JENKINS, M. K. FERBER and C. -K. J. LIN, *ibid.* **76** (1993) 788.
4. A. G. EVANS and E. R. FULLER, *Metall Trans.* **5** (1974) 27.
5. C. J. GILBERT, R. H. DAUSKARDT and R. O. RITCHIE, *J. Amer. Ceram. Soc.* **78** (1995) 2291.
6. A. L. HIGHSMITH and K. L. REIFSNIDER, ASTM STP 775 (1982) 103.
7. R. TALREJA, "Fatigue of composite materials" Technical University of Denmark, Lyngby, Denmark (1985).
8. K. M. PREWO, J. J. BRENNAN and G. K. LAYDEN, *Amer. Ceram. Soc. Bull.* **65** (1986) 305.
9. Z. WANG, C. LAIRD and Z. HASHIN, *J. Mater. Sci.* **26** (1991) 5335.
10. S. SURESH, *J. Hard Materials* **2** (1991) 29.
11. S. SURESH, L. X. HAN and J. J. PETROVICH, *J. Amer. Ceram. Soc.* **71** (1988) C158.
12. L. X. HAN and S. SURESH, *ibid.* **72** (1989) 1233.
13. K. K. CHAWLA, "Ceramic matrix composites" (Chapman & Hall, London, 1993).
14. F. F. LANGE, D. B. MARSHALL and C. F. FOLSOM, US Patent No. 5092948, 1992.
15. D. SHERMAN, J. LEMAITRE and F. A. LECKIE, *Acta Metall. Mater.* **43** (1995) 4483.
16. *Idem*, *ibid.* **43** (1995) 3261.
17. *Idem*, *Eur. J. Mech.* (1996).

Received 23 August 1996
and accepted 17 June 1997

Appendix

The prediction of the loss of stiffness of a cracked laminated system at saturation was developed by

Sherman and co-workers [17]. The normalized effective elastic modulus at that stage was formulated as

$$\frac{E_{\text{sat}}}{E_0} = \left(1 + \xi \frac{1}{\bar{L}/2b} \tanh \bar{L}/2b\right)^{-1} \tag{A.1}$$

where E_0 is the undamaged modulus, $\bar{L}/b$ is the normalized crack spacing at saturation, depends on the elastic moduli and the volume fraction of the constituents and the on interfacial properties [17]. It was calculated to be 3.2. The parameter ξ obeys.

$$\xi = \frac{E_{\text{B}}(f-1)}{E_{\text{D}} f} - f\left(1 + \frac{E_{\text{B}}(f-1)}{E_{\text{D}} f}\right) \tag{A.2}$$